International Journal of
Technology and Emerging Research
ISSN: 3068-109X (online) | ISSN: 3068-1995 (print) | https://www.ioro.org/ijter

Theoretical investigation on mechanism and kinetics of gas phase reaction of HCFC-234fb with HO_2, NO_2 and NO_3 radicals in the atmosphere and fate of alkoxy radical

Narendra Pramanik[a], Debaprasad Dev[*a], Nand Kishor Gour[b], Bhupesh Kumar Mishra[*c]

[a]*Department of Chemistry, Himalayan University, Jullang, Itanagar, Arunachal Pradesh, India*

[b]*Department of Chemical Sciences, Tezpur University, Tezpur, Napaam, Assam – 784 028, India*

[c]*Department of Chemistry, Dera Natung Government College, Itanagar- 791113, Arunachal Pradesh, India*

[*]To whom correspondence should be addressed, Email: bhupesh_chem@rediffmail.com (BKM)

and Email: dchem@gmail.com (DD)

Abstract

1,1-Dichloro-1,3,3,3-tetrafluoropropane, $CF_3CH_2CFCl_2$ commercially known as HCFC-234fb belongs to a class of organic volatile compounds emitted from industry, causes its discharge to the environment by anthropogenic sources. Its extensive presence in industrial processes raises concerns about its environmental impact and leads to the formation of harmful radicals contributing to ozone depletion. In this study, we conducted an in-depth theoretical investigation on the atmospheric oxidation processes of HCFC-234fb initiated by HO_2, NO_2 and NO_3 radicals using the M06-2X functional. Three primary hydrogen abstraction pathways were characterized, each proceeding through the formation of a pre-reactive complex, indicating that the reactions follow an indirect hydrogen abstraction mechanism. The reaction coefficients for H-abstraction channels were calculated and analyzed within the range of 250–450 K by using Canonical Transition State Theory (CTST). Furthermore, the atmospheric fate and primary degradation pathways of the resulting alkoxy radicals $CF_3CH(O)CFCl_2$ were also explored in detail for the first time.

Keywords: HCFC, CTST, DFT, IRC calculation, Rate constant, Alkoxy radical

1. Introduction

Over the past few decades, significant efforts have been made to identify alternatives to these stable chlorofluorocarbons (CFCs) in response to the worldwide concern about the harmful effects of CFCs in the atmosphere. As an alternative to CFCs, a variety of hydrofluorocarbons (HFCs) and hydrochloroflurocarbons (HCFCs) with physicochemical characteristics similar to CFCs have been created and used worldwide [1-3]. The incomplete halogenations of the suggested alternatives are one of their key advantages in terms of their ability to deplete the ozone layer. Since HFCs don't include chlorine, which can catalyze the breakdown of stratospheric ozone, they have been suggested as an environmentally friendly alternative to CFCs in numerous applications [4,5]. However, they do contain alkyl hydrogen, which atmospheric hydroxyl radicals may easily abstract, starting its tropospheric breakdown [6]. Chlorofluorocarbons (CFCs) and hydrochlorofluorocarbons (HCFCs), two ozone-depleting substances (ODSs), are frequently replaced by hydrofluorocarbons (HFCs). These days, they are employed in many different ways, mostly as foam-blowing agents or refrigerants for air conditioning and cooling [7]. Additional applications include solvents, fire safety

© 2026 The Author(s). Published by IORO Publications. This is an open-access article distributed under the terms of the Creative Commons Attribution 4.0 International License (CC BY 4.0) (https://creativecommons.org/licenses/by/4.0/), which permits use, distribution, and reproduction in any medium, provided the original author and source are credited, a link to the license is provided, and any changes are indicated.

systems, metered dose inhalers, and aerosol spray cans. The Montreal Protocol, which is frequently cited as a singular instance of an international agreement that effectively prevented an environmental catastrophe, is phasing out ODSs. Due to presence of C–F bonds leads to intense IR absorptions within the atmospheric window (750–1250 cm^{-1}), these HFCs are making a growing contribution to global radiative forcing, [8]. The primary mechanisms for these HFCs degradation in the atmosphere may be initiated in coastal locations by reactions with OH radicals and Cl atoms. To ascertain their environmental impact on the quality of air and other matrices, kinetic and mechanistic analyses of the degradation of these HFCs triggered by interaction with OH radicals are pertinent.

Based on the available literature, a few determinations of the rate constant for the reaction of HCFC-234fb with atmospheric oxidants have been reported. In this regard, Barry et al. [9] reported the Rate coefficients for the gas-phase reactions of OH radical and Cl atom with HCFc-234fb and reported experimental rate constant values as k_{OH} (8.0 ± 3.0) 10^{-16} cm^3 $molecule^{-1}$ s^{-1} and k_{Cl} (3.5 ± 1.5) 10^{-17} cm^3 $molecule^{-1}$ s^{-1}. In another study, Andersen et al. [10] reported the rate constant of k_{OH} (2.9 ± 0.8) 10^{-15} cm^3 $molecule^{-1}$ s^{-1} and k_{Cl} (2.3 ± 0.6) 10^{-17} cm^3 $molecule^{-1}$ s^{-1} for the reaction of HCFC-234fb with OH and Cl atom Recently. Changmai et al [11] explored the reactivity of HCFC-234fb with OH radical and Cl atom by means of theoretical methods. No qualitative and quantitative products studies are currently available for HO_2, NO_2 and NO_3 initiated degradation of HCFC-234fb neither experimentally nor theoretical calculations. In addition, there are not previous studies of the products distribution for the degradation mechanism of alkoxy radical produced by HCFC-234fb in atmosphere. A well-defined theoretical study is very desirable in order to identify the feasible mechanism and gain a better grasp of the kinetics of the title reaction. In order to gain a more thorough knowledge of the title reaction, we presented a thorough theoretical analysis of the hydrogen abstraction reaction between HCFC-234fb and atmospheric oxidants as an addition to the experiments.

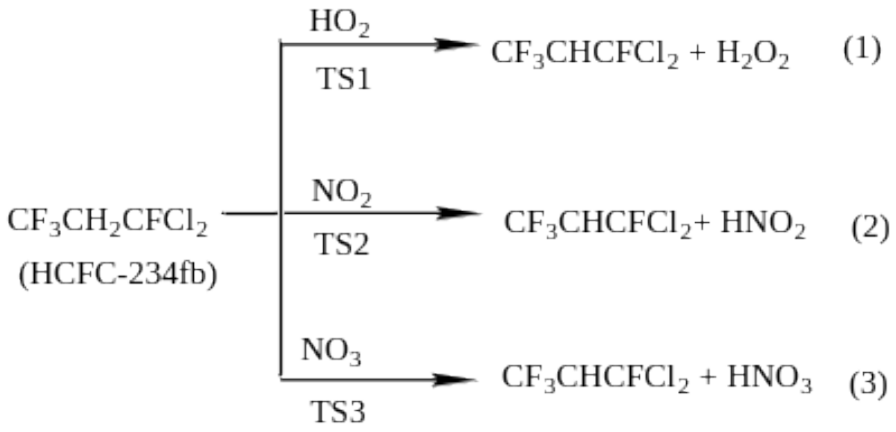

As far as we are aware, no theoretical investigation has been carried out to clarify the dissociative routes of the $CF_3CH(O)CFCl_2$ radicals. We have considered four prospective pathways of decomposition of $CF_3CH(O)CFCl_2$ radical that engross bond scissions and oxidation processes. These are represented as follows:

$$CF_3CH(O^{\bullet})CFCl_2 + O_2 \longrightarrow CF_3C(O)CFCl_2 + HO_2 \quad (4)$$

$$\longrightarrow CF_3 + CH(O^{\bullet})CFCl_2 \quad (5)$$

$$\longrightarrow CF_3CH(O) + CFCl_2 \quad (6)$$

$$\longrightarrow CF_3C(O)CFCl_2 + H \quad (7)$$

Since haloalkoxy radicals are intriguing intermediates in the atmospheric oxidation of halogenated hydrocarbons, their chemistry has been the focus of in-depth experimental and theoretical research [12-21]. Our goal in using the theoretical tools is to (i) learn more about what happens to these alkoxy radicals and (ii) investigate the significance of the other possible paths that these radicals may take.

2. Computational methods

We performed all the computational quantum calculations work using Gaussian 09 program package [22]. The electronic structures of the reactants (Rs), reaction complexes (RCs), product complexes (PCs), transition states (TSs) and products (Ps) were optimized using hybrid density functional M06-2X [23] along with 6-31+G(d,p) basis set. Further, we were carried out frequency calculations of all the optimized species using the same M06-2X /6-31+G(d,p) method. From frequency analysis, we found that for stable species, these were no imaginary frequencies which ensure these molecules to have either local or global minima energies while for the TSs, we found one imaginary frequency to ensure it has maxima along the reaction coordinate. Based on previous reports [24-29] it has been demonstrated that this hybrid density functional, M06-2X, produces satisfactory results for thermochemistry and kinetics for the hydrogen abstraction reactions for the volatile organic compounds. In order to validate to correct TSs which was really connecting the reactant and product species, we performed IRC calculation [30] throughout the reaction channels.

3. Results and discussion

For the reaction channels (1-3), we have located three transition states viz., TS1, TS2, and TS3, respectively on the relaxed potential energy surface. Pre-reactive complexes (RC1, RC2, and RC3) have been found in the entrance channel for reactions (1-3) in the current investigation. The exit channel also contains product complexes, referred to as PC1, PC2 and PC3, with energies lower than the corresponding products before the final product is distributed. Therefore, it is clear that the reaction channels (1-3) may employ indirect procedures. The least energy path was used to find stationary spots on a relaxed potential energy surface. Figure 1 depicts the electronic structure of the optimized geometry of the reactant, products, reaction complexes, product complexes, and transition states that were produced at the M06-2X/6-31+G(d,p) level.

At the M06-2X/6-311+G(d,p) level, the precise thermodynamic calculations for reaction enthalpies ($\Delta_r H^\circ$) and free energies ($\Delta_r G^\circ$) at 298 K for loss processes (13) are documented in Table 1. These thermodynamic functions were determined with thermal corrections to the energy at 298 K. It is evident from Table 1 that the reaction channel 3 i.e. hydrogen abstraction by NO3 radical are more feasible pathways due to its exergonic nature. The optimized structures of the pre-reaction complexes (RC1, RC2 and RC3) and post -reaction complexes (PC1, PC2 and PC3) are shown in Fig. 1. As shown in the reaction energy profile diagram in Fig. 2, three pre-reaction complexes were located at the entry point of three reaction channels originated by the interaction of HCFC-234fb with HO_2, NO_2 and NO_3 radicals. On other hand, three post-reaction complexes (PC1, PC2 and PC3) were found at the exit channels of the reaction. The RC and PC complexes are formed due to weak interaction through C–H…..O and H…..F/O hydrogen bonding,

Visualization of the optimized structures of TS1 for reaction channel 1 i.e. hydrogen abstraction by HO_2 radical, the breaking CH bond length (C3-H6) is elongated from 1.092 to 1.441 Å (31.95%) than the observed CH bond length in the isolated HCFC-234fb molecule, According to the TS2 analysis conducted for reaction channel 2, the C–H (C3–H6) bond length has elongated from 1.092 to 1.258 Å. The length of the breaking C-H bond (C3-H6) in transition state TS3 for reaction 3 is also found to be 13.91% greater than the measured C-H bond length in the isolated molecule. Table 2 presents the results of the harmonic vibrational frequency

calculation at the M06-2X/6-311+G(d,p) level. Each transition state has one imaginary frequency due to its first order saddle point character, while the analysis of the harmonic vibrational frequency of minima including reactants, pre-reactant complexes (RCs), product complexes (PCs), and products revealed no imaginary frequency (NIMAG = 0). The C3–H6 and O12–H6 stretching modes are represented by the imaginary frequency 1557 cm^{1} for transition state TS1 regarding reaction channel (1). This also shows a considerable curvature in the potential energy surface (PES) surrounding the transition state. The imaginary frequency for the hydrogen abstraction by NO_2 radical involving TS2 is determined to be 1797 cm^{1}, which corresponds to the stretching modes for hydrogen transfer reactions H6–O12 and C3–H6. At the M06-2X/6-31+G(d,p) level, the transition states TS3 for NO_3 initiated hydrogen abstraction were optimized with a single imaginary frequency, which was found to be 1628 cm^{1}.

The representation of the normal-mode corresponding to the calculated imaginary frequencies shows a clear transition state geometry connecting reactants and products during transition. To further ascertain whether a transition state exists on the potential energy surface, the intrinsic reaction coordinate (IRC) calculation [30] is performed at the same theoretical level using the Gonzalez-Schlegel steepest descent path in the mass-weighted Cartesian coordinates with a step size of 0.01 ($amu^{1/2}$- bohr). Additional proof that the transition state truly connects the intended reactant and product along the corresponding potential energy surface is given by the results of IRC calculations, which are shown in Fig. 3. Table 3 summarizes the relative energy of each optimized geometry used in this study, which was determined using the M06-2X/6-311+G(d,p) method. We employed the species optimal geometries, M06-2X/6-311+G(d,p), for the energetic computation. Using frequency calculation data at the M06-2X/6-311+G(d,p) level of theory, optimization was carried out to find each species' zero-point energy. Zero-point energy (ZPE) corrected total energies were calculated with a scale factor of 0.967 [31]. Fig. 2 shows a schematic potential energy profile of that was acquired at the M06-2X level using zero-point energy (ZPE) adjustments. Zero-point energy corrected total energy has been used in the energy diagram's development. The ground state energy of HCFC-234fb + HO_2/NO_2/NO_3 radicals, which includes ZPE, is plotted against these energies, with zero being used randomly. For TS1, TS2 and TS3, the energy barrier determined at the M06-2X/6-31+G(d,p) level is 21.47, 37.62, and 8.96 kcal mol^{1}, respectively. It can see from this Table 3 that the barrier heights for abstraction of hydrogen atom by NO_3 radical is lowest in compare to other two reaction channels 1 and 2. According to the obtained barrier heights, we would expect that reactivity of HCFC-234fb is the highest towards NO_3 radical while reactivity of NO_2 radical is the lowest one.

3.1. *Kinetics calculation*

The conventional transition state theory (CTST) [32] and Eckart's tunneling correction [33] were used to calculate the rate coefficient values for various reaction channels spanning the 250–450 K temperature range using the following formula.

$$k=(T)\frac{k_B T}{h}\frac{Q^{\ddagger}_{TS}}{Q_R}\exp\frac{-\Delta E}{RT}(8)$$

The represents symmetry factor whereas tunneling correction factor at temperature T is represented by the symbol (T). The total partition functions (per unit volume) for the reactants and transition states are denoted by Q_R and ,, respectively. R stands for the universal gas constant, k_B for the Boltzmann constant, h for Planck's constant, and E for the barrier height incorporating zero point energy correction. The obtained rate coefficients in the temperature range of 250 – 450 K for reaction pathways (1–3) are recorded in Table 4. At 298 K, our calculated rate constants for TS1, TS2 and TS3 were found to be 5.80×10^{30} , 5.93×10^{41} and 2.01×10^{20} cm^{3} $molecule^{1}$ s^{-1} respectively at M06-2X/6-31+G(d,p) level of theory. There is no previous

experimental or computational study on reactivity of HCFc-234fb with these radicals to compare our results. Thus it may be concluded that H-abstraction reaction by NO_3 radical, i.e., reaction channel 3 is important consumption channels for HCFC-234fb leading to the formation of $CF_3CHCFCl_2$ and HNO_3.

3.2. *Atmospheric fate of alkoxy radical*

In this section, we will investigate the degradation pathways of the alkoxy radical The $CF_3CH(O)CFCl_2$ produced from the hydrogen abstraction of HCFC-234fb molecule. A mechanism for its decomposition in atmosphere is anticipated through reaction channels (4–7). The thermodynamic parameter like reaction enthalpies ($\Delta_rH^\circ_{298}$) and free energies ($\Delta_rG^\circ_{298}$) related to reaction channels (47) carried out at the M06-2X/6-311+G(d,p) level are recorded in Table 1. It can be noted that reaction channel 7 proceed with positive free energy changes ($\Delta_rG^\circ_{298}$> 0), according to the results obtained during the thermodynamic calculation performed in this study. Therefore, it may be concluded that reaction channel 7 is not thermodynamically competitive with other channels. We have optimized four transition states labeled as TS4, TS5, TS6 and TS7 on potential energy surface for the decomposition pathways of alkoxy radical. Table 5 records the harmonic vibrational frequencies of the alkoxy radical, products, and transition states involved in reactions (4–7). The result obtained from frequency calculation shows that the transition states are characterized by the occurrence of only one imaginary frequency obtained at 1707, 357, 405 and 909 cm^1 for TS4, TS5, TS6 and TS7, respectively. The optimized geometries of alkoxy radical, transition states (TS4, TS5, TS6 and TS7) and products obtained at the M06-2X/6-311+G(d,p) level are displayed in Fig. 4 with bond length (Å).

The alkoxy radical undergoes oxidative pathways involving TS4 on interaction with O_2, resulting in the creation of a carbonyl compound and HO_2 radical. The CH (C3-H5) bond is extended from 1.098 to 1.302 Å (18%) in the optimized structure of TS4 with a simultaneous shrinkage of CO (C3O11) bond from 1.374 to 1.257Å. For CC bond fission pathways, we have considered two reaction channels 5 and 6 involving TS5 and TS6. The electronic structure visualization for TS5 shows that the breaking distance C3–C2 increases from 1.554 to 2.145 Å at the transition point leading to formation of CF_3 and $CFCl_2CH(O)$ radical. For another CC bond decomposition pathways, transition state thus located is designated as TS6. The electronic structure of TS6 obtained during the present study reveals the elongation of C–C (C3C1) bond length from 1.546 to 2.037 Å leading to the formation of $CF_3CH(O)$ and $CFCl_2$ radical. The transition state TS7 which corresponds to the breaking of the C–H bond reveals the elongation of C–H (C3H5) bond length from 1.098 to 1.850 Å with a simultaneous shrinkage of the CO (C3O11) bond from 1.374 to 1.199 Å. The existence of these transition states on the potential energy surface are further ascertained by intrinsic IRC calculation [30] performed at the same level of theory. The associated energy barriers corresponding to reactions (47) calculated at M06-2X level of theory are recorded in Table 6. A potential energy diagram for the decomposition channels is constructed with the results obtained at the M06-2X/ 6-311+G(d,p) level and is shown in Fig. 5. In the construction of energy diagram zero-point corrected total energy data are utilized and the sum of the zero point corrected ground state energies of $CF_3CH(O)CFCl_2$ and O_2 is arbitrarily taken as zero. The zero-point energy corrected energy barriers corresponding to reactions (47) yields a value of 4.29, 14.34, 7.89 and 23.43 kcal mol^{-1} for TS4, TS5, TS6 and TS7, respectively. The energy barriers corresponding to reactions (47) show that the energy barrier for H-abstraction reaction of $CF_3CH(O)CFCl_2$ radical with molecular O_2 is considerably lower than that for other decomposition pathways and the dominance of the oxidative pathways of this alkoxy radical in the atmosphere is thus envisioned leading to the formation of $CF_3C(O)CFCl_2$ and HO_2 radical.

4. Conclusions

In present study we have explored the atmospheric and environmental consequence of HCFC-234fb molecule initiated by HO_2, NO_2 and NO_3 radical by employing M06-2X/6-311+G(d,p) level of theory. For that, we have identified three reaction channels which follow an indirect path through the formation of pre- and post-reaction complexes on the potential energy surface. In this manuscript, we applied an effective as well as reliable computational strategy for predicting accurately the tropospheric reactivity of the titled molecule and atmospheric implications. The thermodynamic and kinetic studies suggested that the abstraction of H-atoms by NO_3 radical from HCFC-234fb, is the most important pathway in compare to other HO_2 and NO_2 radical. The reaction coefficients for H-abstraction channels were calculated within the range of 250–450 K by using Canonical Transition State Theory (CTST). The thermal rate constant for reactivity with NO_3 radical is found to be 2.01×10^{20} cm^3 $molecule^1$ s^1 at 298 K. Furthermore, this study proposes detailed degradation pathways for the alkoxy radicals derived from HCFc-234fb. Based on the results obtained in this study, it can be emphasized that the reaction with O_2 is the main atmospheric fate for decomposition of $CF_3CH(O)CFCl_2$ radical. These data can be useful for further thermo-kinetic modeling of other reactions involving these species.

Acknowledgment

The authors acknowledge financial support from the Department of Science and Technology, New Delhi in the form of project under DST-SERB CRG scheme (CRG/2023/002561).

CRediT authorship contribution statement

Narendra Pramanik: Writing – review & editing, Visualization. Nand Kishor Gour: Writing – review & editing, Visualization. Debaprasad Dev: Writing – review & editing, Visualization, Validation, Supervision. Bhupesh Kumar Mishra: Conceptualization, Data Creation, Validation, Supervision.

Competing interests

The author declares no competing interests.

REFERENCES

[1] S. Urata, A. Takada, T. Uchimaru, A.K. Chandra. Rate constants estimation for the reaction of hydrofluorocarbons and hydrofluoroethers with OH radicals. Chem. Phys. Lett. 368 (2003) 215–223. http://10.1016/S0009-2614(02)01718-9

[2] M. J. Molina and F. S. Rowland. Stratospheric sink for chlorofluoromethanes:chlorine atom-catalysed destruction of ozone. Nature 249 (1974) 810-812. https://doi.org/10.1038/249810a0

[3] A. McCulloch. CFC and Halon replacements in the environment. J. Fluorine Chem. 100 (1–2) (1999) 163-173. https://doi.org/10.1016/S0022-1139(99)00198-0

[4] D. J. Weubbles. Chlorocarbon emission scenarios: Potential impact on stratospheric ozone. J. Geophys. Res. 88(C2) (1983) 1433-1443. https://doi.org/10.1029/JC088iC02p01433

[5] V. Papadimitriou. Prospective Primary Teachers' Understanding of Climate Change, Greenhouse Effect, and Ozone Layer Depletion, J. Sci. Educ. Technol. 13(2) (2004) 299–307. https://www.jstor.org/stable/40188791

[6] R. P. Wayne. Chemistry of Atmospheres; Clarendon press: Oxford, (2001).

[7] H. Flerlage, J. M. G. Velders and J. Boer. A review of bottom-up and top-down emission estimates of hydrofluorocarbons (HFCs) in different parts of the world. Chemosphere 283 (2021) 131208. https://doi.org/10.1016/j.chemosphere.2021.131208

[8] S. A. Montzka, G. J. M Velders, P. B. Krummel, J. Mühle, V. L. Orkin, S. Park, N. Shah and H. Walter-Terrinoni. Hydrofluorocarbons: Chapter 2. Scientific Assessment of Ozone Depletion: 2018. Global Ozone Research and Monitoring Project-Report No. 58, Geneva, Switzerland (2018).

[9] M. P. S. Andersen, M. Frausig and O. J. Nielsen. Atmospheric chemistry of CCl2FCH2CF3 (HCFC-234fb): Kinetics and mechanism of reactions with Cl atoms and OH radicals. Int. J. Chem. Kinet. 55(2) (2023) 63-71. https://doi.org/10.1002/kin.21615

[10] R. R. Changmai, S. R. Daimari, A. K. Yadav and M. Sarma. Atmospheric oxidation pathways of CF3CH2CFCl2(HCFC-234fb) with OH-radicals and Cl-atoms: insights into the mechanism, thermodynamics,and kinetics. Phys. Chem. Chem. Phys. 26(35) (2024) 23363-23371. https://doi.org/10.1039/d4cp01643b

[11] Y. Ninomiya, M. Kawasaki, A. Guschin, L. T. Molina, M. J. Molina and T. J. Wallington. Atmospheric Chemistry of n-C3F7OCH3: Reaction with OH Radicals and Cl Atoms and Atmospheric Fate of n-C3F7OCH2O(•) Radicals. Environ. Sci. Technol. 34 (14) (2000) 2973-2978. https://doi.org/10.1021/es991449z

[12] J. J. Orlando, G. S. Tyndall and T. J. Wallington. The Atmospheric Chemistry of Alkoxy Radicals. Chem. Rev. 103(12) (2003) 4657-4690. https://doi.org/10.1021/cr020527p

[13] M. A. Ferenac, A. J. Davis, A. S. Holloway and T.S. Dibble. Isomerization and Decomposition Reactions of Primary Alkoxy Radicals Derived from Oxygenated Solvents. J. Phys. Chem. A. 107(1) (2003) 63-72. https://doi.org/10.1021/jp0262923

[14] W. Deng, A. J. Davis, L. Zhang, D. R. Katz and T. S. Dibble. Direct Kinetic Studies of Reactions of 3-Pentoxy Radicals with NO and O2. J. Phys. Chem. A. 105 (39) (2001) 8985-8990. https://doi:10.1021/jp011875i

[15] B. K. Mishra, M. Lily; A. K. Chakrabartty; D. Bhattacharjee; R. C. Deka, and A. K. Chandra. Theoretical investigation of atmospheric chemistry of volatile anaesthetic sevoflurane: reactions with the OH radicals and atmospheric fate of the alkoxy radical (CF3)2CHOCHFO: thermal decomposition vs. oxidation. New J. Chem. 38(7) (2014) 2813-2822. https://doi.org/10.1039/c3nj01408h

[16] Singh, H.J., Mishra, B.K., and Gour, N.K. Theoretical studies of decomposition kinetics of CF3CCl2O radical. Theoretical Chemistry Account, 125 (2010) 57-64. https://doi.org/10.1007/s00214-009-0659-0

[17] Bhattacharjee, D., Mishra, B.K., and Deka, R.C. Theoretical insight on atmospheric chemistry of HFE-365mcf3: reactions with OH radicals, atmospheric lifetime, and fate of alkoxy radicals (CF3CF2CH(O•)OCH3/CF3CF2CH2OCH2O•). J. Mol. Model. 21 (2015) 69. https://doi.org/10.1007/s00894-015-2629-x

[18] Tayum, N., Gour, N.K., Murugan, A., and Mishra, B.K. Theoretical Insights into the Reactivity of M2CAA with OH Radicals and the Fate of Resulting Alkoxy Intermediates. ChemistrySelect, 11(1) 2026 e04798. https://doi.org/10.1002/slct.202504798

[19] Vereecken, L and Francisco, J. S. Theoretical studies of atmospheric reaction mechanisms in the troposphere. Chem. Soc. Rev. 41(19) (2012) 6259-6293. https://doi.org/10.1039/c2cs35070j

[20] Mishra, B.K. Theoretical investigation on the atmospheric fate of the CF3C(O)OCH(O)CF3 radical: alpha-ester rearrangement vs. oxidation. RSC Advances 4(32) (2014) 16759-16764. https://doi.org/10.1039/c4ra00881b

[21] M. J. Frisch. et al. Gaussian 09 (Revision B.01); Gaussian Inc.; Wallingford, CT. (2009).

[22] Zhao, Y and Truhlar, D.G. The M06 suite of density functionals for main group thermochemistry, thermochemical kinetics, noncovalent interactions, excited states, and transition elements: two new functionals and systematic testing of four M06-class functionals and 12 other functional. Theor. Chem. Acc. 120 (2008) 215-241. https://doi.org/10.1007/s00214-007-0310-x

[23] N. K. Gour, K. Borthakur, S. Paul, and R. C. Deka. Tropospheric degradation of 2-fluoropropene (CH3CFdouble bondCH2) initiated by hydroxyl radical: Reaction mechanisms, kinetics and atmospheric implications from DFT study. Chemosphere 238 (2020) 124556. https://doi.org/10.1016/j.chemosphere.2019.124556

[24] M. Lily, B. K . Mishra and A. K. Chandra. Kinetics, mechanism and thermochemistry of the gas phase reactions of CF3CH2OCH2CF3 with OH radicals: A theoretical study. J. Fluor. Chem. 161 (2014) 51-59. https://doi.org/10.1016/j.jfluchem.2014.02.009

[25] N. Tayum, A. Murugan, R. C. Deka, N. K. Gour, and B. K. Mishra. The molecular level study of the fate of the CH3CH2C(O)OCH(O)CH3 radical derived from ethyl propionate. Molecular Simulation, 49(7) (2023) 711-719. https://doi.org/10.1080/08927022.2023.2189975

[26] B. Baidya, M. Lily, D. Patgiri, S. Hynniewta, and A. K. Chandra. CHF2CF2OCHF2: conformational analysis and direct dynamics study of its reaction with Cl atoms and atmospheric fate. New J. Chem. 44(11) (2020) 4276-4284. https://doi.org/10.1039/C9NJ06069C

[27] S. Paul, B. K. Mishra, S. D. Baruah, and R. C. Deka. Atmospheric oxidation of HFE-7300 [n-C2F5CF(OCH3)CF(CF3)2] initiated by •OH/Cl oxidants and subsequent degradation of its product radical: a DFT approach. Env. Sci. Poll. Res., 27 (2020) 907-920. https://doi.org/10.1007/s11356-019-06975-1

[28] N. K. Gour, B. K. Mishra, P. J. Sarma, P. Begum, and R. C. Deka. Tropospheric degradation of HFE-7500[n-C3F7CF(OCH2CH3)CF(CF3)2] initiated by OH radicals and Fate of alkoxy radical [n-C3F7CF(OCH(Oradical dot)CH3)CF(CF3)2]: A DFT investigation. J. Fluor. Chem. 204 (2017) 11-17. https://doi.org/10.1016/j.jfluchem.2017.09.010

[29] C. Gonzalez and H. B. Schlegel. An improved algorithm for reaction path following. J. Chem. Phys. 90 (1989) 2154-2161. https://doi.org/10.1063/1.456010

[30] I. M. Alecu, J. Zheng, Y. Zhao, and D. G. Truhlar. Computational Thermochemistry: Scale Factor Databases and Scale Factors for Vibrational Frequencies Obtained from Electronic Model Chemistries. J. Chem. Theory Comput., 6(9) (2010) 2872-2887. https://doi.org/10.1021/ct100326h

[31] K. J. Laidler. Chemical Kinetics, 3rd edn. Pearson Education, New Delhi (2004).

[32] R. Xiao, M. Noerpel, H. L. Luk, Z. Wei, and R. Spinney. Thermodynamic and kinetic study of ibuprofen with hydroxyl radical: A density functional theory approach. Int. J. Quant. Chem. 114(1) (2014)74-83. https://doi.org/10.1002/qua.24518

Table 1 Thermochemical data (kcal mol^{1}.) for reaction channels (17) calculated at M06-2X/6-311+G(d,p) level of theory at 298 K.

Reaction channels	$\Delta_r H°_{298}$	$\Delta_r G°_{298}$
Reaction 1	16.24	15.22
Reaction 2	21.93	21.05
Reaction 3	-6.42	-6.81
Reaction 4	-28.09	-29.68
Reaction 5	9.42	-4.506
Reaction 6	3.79	-10.29
Reaction 7	18.98	10.92

Table 2 Harmonic vibrational frequencies of reactants, transition states and products at M06-2X/6-311+G(d,p) level of theory.

Species	Vibrational Frequencies (cm^{-1})
$CF_3CH_2CFCl_2$	33, 102, 144, 238, 245, 304, 349, 380, 415, 488, 534, 546, 657, 696, 778, 886, 979, 1091, 1153, 1194, 1223, 1310, 1340, 1436, 1467, 3100, 3163
TS1	1557i, 41, 45, 68, 93, 122, 138, 182, 233, 248, 306, 346, 366, 367, 438, 487, 533, 555, 644, 675, 706, 760, 902, 910, 1043, 1079, 1161, 1170, 1222, 1270, 1287, 1404, 1435, 1476, 3162, 3796
TS2	1797i, 38, 39, 63, 80, 119, 140, 159, 198, 238, 250, 300, 319, 350, 397, 489, 511, 542, 569, 655, 703, 736, 766, 821, 902, 982, 1100, 1151, 1201, 1219, 1236, 1310, 1346, 1431, 1791, 3155
TS3	1628i, 37, 42, 44, 69, 96, 124, 130, 154, 220, 247, 298, 314, 352, 396, 488, 500, 540, 565, 671, 696, 706, 766, 808, 817, 901, 943, 976, 1100, 1143, 1148, 1223, 1254, 1311, 1359, 1401, 1417, 1770, 3142
RC1	26, 55, 58, 99, 105, 125, 141, 187, 242, 246, 304, 339, 349, 384, 419, 489, 536, 546, 658, 695, 788, 885, 980, 1054, 1147, 1202, 1219, 1282, 1310, 1340, 1435, 1464, 1488, 3095, 3157, 3656
RC2	23, 38, 42, 59, 74, 96, 108, 138, 140, 239, 245, 304, 349, 380, 415, 488, 535, 545, 657, 695, 783, 792, 887, 978, 1083, 1150, 1198, 1219, 1311, 1339, 1433, 1460, 1477, 1805, 3095, 3155
RC3	24, 38, 44, 53, 79, 80, 115, 129, 141, 240, 246, 304, 350, 381, 386, 419, 487, 537, 550, 660, 690, 694, 791, 818, 876, 887, 985, 1088, 1156, 1197, 1210, 1313, 1347, 1391, 1440, 1465, 1689, 3101, 3163
PC1	41, 55, 60, 65, 92, 124, 132, 147, 156, 243, 250, 304, 350, 383, 414, 430, 483, 505, 534, 612, 665, 704, 813, 909, 1034, 1080, 1166, 1186, 1231, 1305, 1336, 1439, 1486, 3245, 3840, 3859
PC2	37, 45, 59, 76, 86, 100, 122, 143, 156, 239, 248, 303, 326, 349, 389, 479, 492, 532, 598, 624, 665, 702, 730, 806, 904, 955, 1104, 1154, 1166, 1247, 1302, 1378, 1442, 1844, 3270, 3807
PC3	23, 53, 64, 66, 75, 87, 106, 127, 141, 238, 248, 301, 350, 370, 392, 482, 495, 533, 569, 607, 637, 658, 705, 719, 798, 826, 908, 999, 1103, 1163, 1201, 1236, 1298, 1390, 1432, 1439, 1823, 3260, 3716
HO_2	1257, 1460, 3708
NO_2	786, 1472, 1796
NO_3	341, 689, 808, 844, 1385, 1682
$CF_3CHCFCl_2$ (P)	48, 71, 143, 224, 243, 274, 301, 349, 388, 479, 489, 533, 597, 661, 703, 810, 908, 1097, 1157, 1188, 1234, 1303, 1436, 3238
H_2O_2	417, 1037, 1345, 1499, 3859, 3860
HNO_2	608, 707, 911, 1341, 1858, 3831
HNO_3	464, 624, 709, 815, 980, 1361, 1429, 1831, 3796

Table 3 Relative energies (in kcal mol^1) with zero-point energy correction for the reactants, reaction complexes, transition states, product complexes and products at M06-2X/6-311+G(d,p) level of theory.

Species	M06-2X/6-311+G(d,p)
HCFC-234fb + HO_2/NO_2/NO_3	0.00
RC1	-5.29
RC2	-2.79
RC3	-3.72
TS1	21.47
TS2	37.62
TS3	8.96
PC1	9.86
PC2	16.79
PC3	-12.04
P1 + H_2O_2	15.85
P2 + HNO_2	21.62
P3 + HNO_3	-6.62

Table 4: Rate constants of different reaction channels and overall rate constant (in cm^3 $molecule^1$ s^1) within the temperature range of 250450 K at M06-2X/6-311+G(d,p) level of theory.

Rate constant	250 K	298.15 K	300 K	350 K	400 K	450 K
k_1	6.63×10^{-33}	5.80×10^{-30}	7.22×10^{-30}	1.14×10^{-27}	5.31×10^{-26}	1.08×10^{-24}
k_2	2.00×10^{-45}	5.93×10^{-41}	8.30×10^{-41}	2.56×10^{-37}	1.34×10^{-34}	1.92×10^{-32}
k_3	7.51×10^{-21}	2.01×10^{-20}	2.09×10^{-20}	6.70×10^{-20}	2.03×10^{-19}	5.30×10^{-19}

Table 5 Harmonic vibrational frequencies of alkoxy radical, transition states and products at M06-2X/6-311+G(d,p) level of theory.

Species	Vibrational Frequencies (cm^{-1})
$CF_3CH(O^•)CFCl_2$	37, 95, 149, 200, 236, 257, 299, 330, 376, 404, 458, 501, 540, 592, 703, 734, 887, 911, 1051, 1115, 1163, 1222, 1256, 1298, 1362, 1830, 3073
TS4	1707i, 35, 59,62, 127, 142, 190, 204, 218, 242, 296, 307, 343, 372, 397, 472, 494, 540, 558, 615, 742, 766, 894, 909, 1052, 1081, 1186, 1256, 1264, 1308, 1397, 1592, 1670
TS5	357i, 47, 61, 109, 158, 183, 190, 253, 278, 374, 394, 415, 503, 533, 542, 663, 675, 900, 932, 1039, 1063, 1161, 1323, 1346, 1368, 1628, 3012
TS6	405i, 48, 65, 124, 174, 249, 268, 312, 340, 403, 452, 494, 543, 568, 615, 714, 862, 914, 1010, 1182, 1212, 1230, 1318, 1359, 1569, 2997
TS7	909i, 50, 73, 146, 184, 238, 266, 297, 328, 371, 393, 469, 505, 528, 535, 571, 604, 727, 754, 889, 918, 1063, 1187, 1237, 1280, 1325, 1799
$CF_3C(O)CFCl_2$	42, 68, 145, 150, 230, 242, 286, 332, 378, 394, 473, 503, 528, 606, 732, 758, 891, 913, 1074, 1211, 1242, 1285, 1344, 1938
HO_2	1257, 1460, 3707
CF_3	519, 520, 707, 1112, 1299, 1305
$CH(O)CFCl_2$	90, 211, 255, 307, 388, 406, 555, 636, 839, 1031, 1095, 1156, 1388, 1919, 3028
$CF_3CH(O)$	91, 259, 321, 437, 535, 538, 719, 863, 995, 1228, 1240, 1348, 1415, 1920, 3036
$CFCl_2$	284, 389, 456, 612, 926, 1210

Table 6 Relative energies (in kcal mol^1) with zero-point energy correction for reaction channels (4-7) at M06-2X/6-311+G(d,p) level of theory.

Species	M06-2X/6311+G(d,p)
TS4 (Reaction with O_2)	4.29
TS5 (C-C bond fission)	14.34
TS6 (C-C bond fission)	7.89
TS7 (C-H bond fission)	23.43

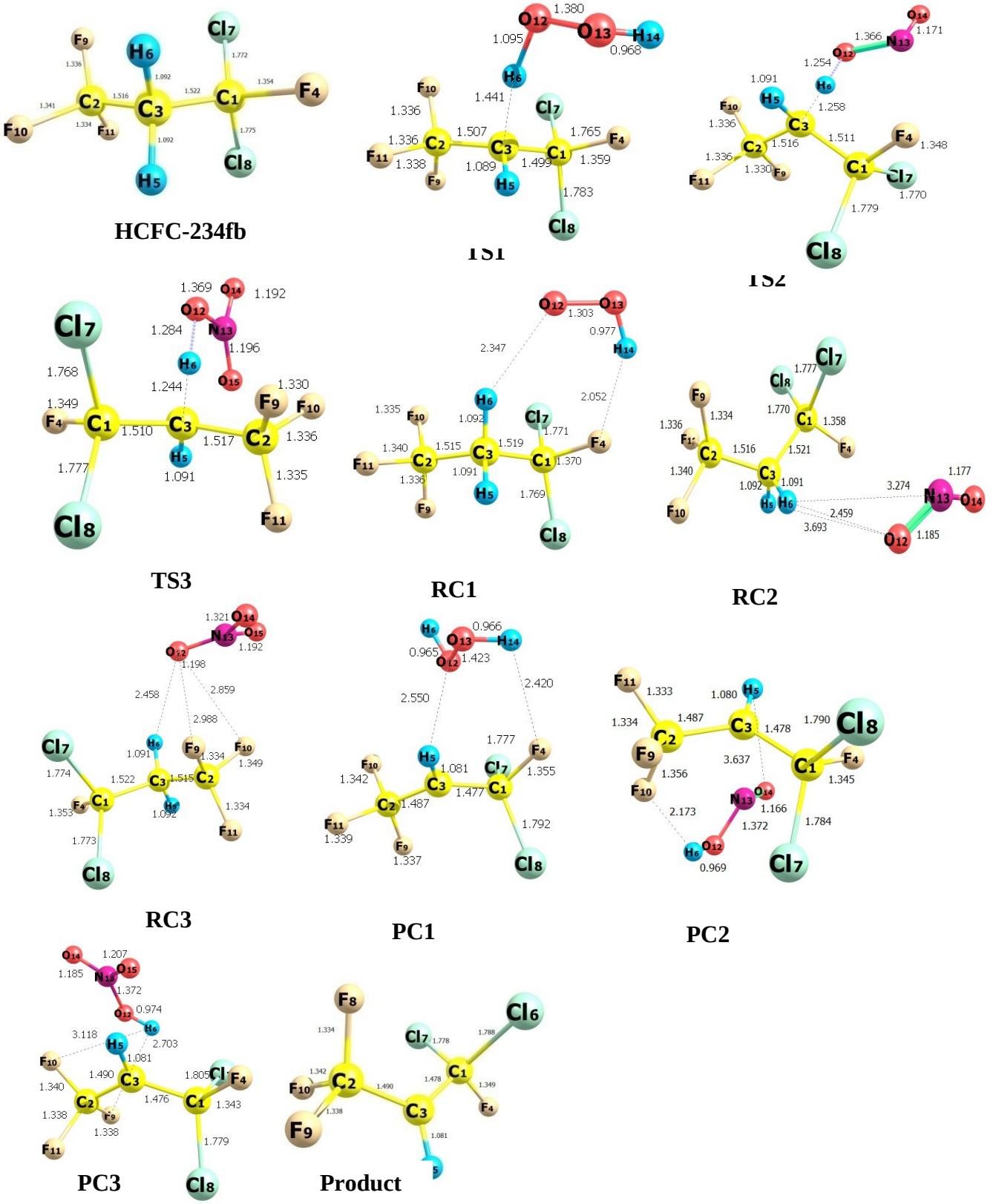

Fig. 1: Optimized geometries of E2CAA, transition states and reactive complexes at M06-2X/6-311+G(d,p)level. Bond lengths are in Angstroms.

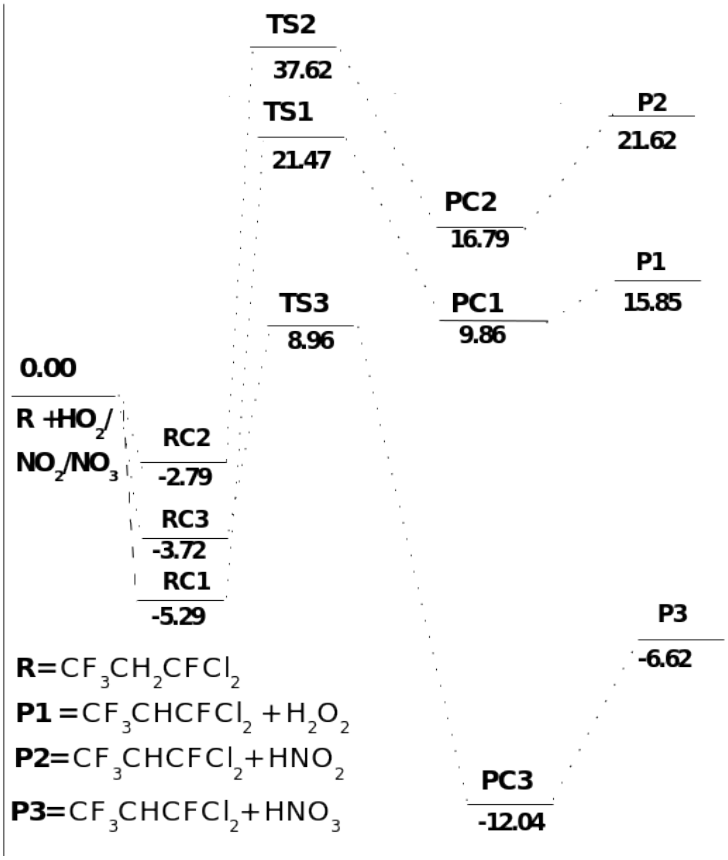

Fig. 2: Schematic potential energy diagram at M06-2X/6-311+G(d,p) level. Relative energies for reaction channels (1-3) with ZPE are expressed in kcal mol[1].

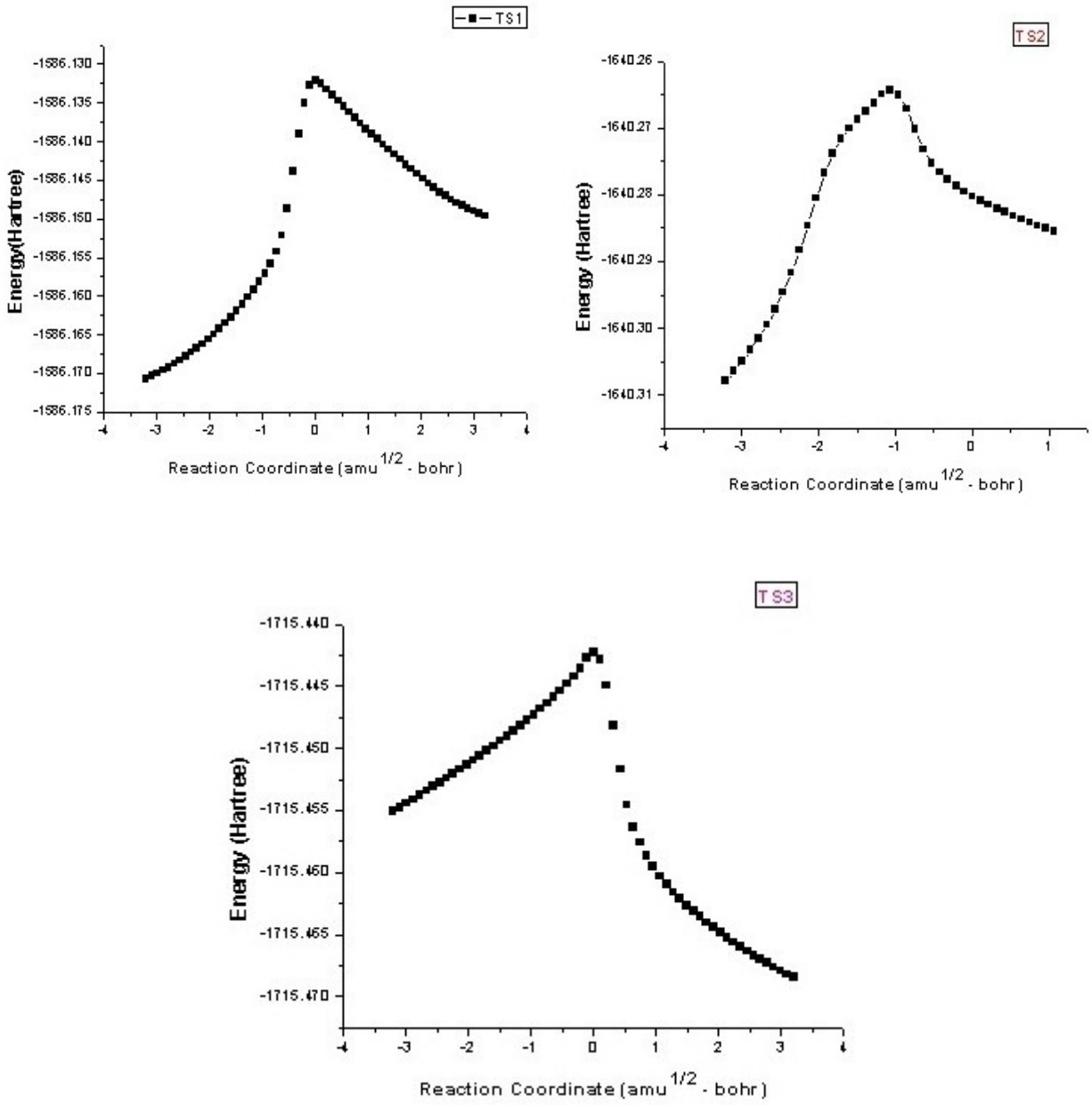

Fig. 3: IRC plot performed for transition states TS1, TS2 and TS3 for reaction channels (1-3) at M06-2X/6-311+G(d,p) level of theory.

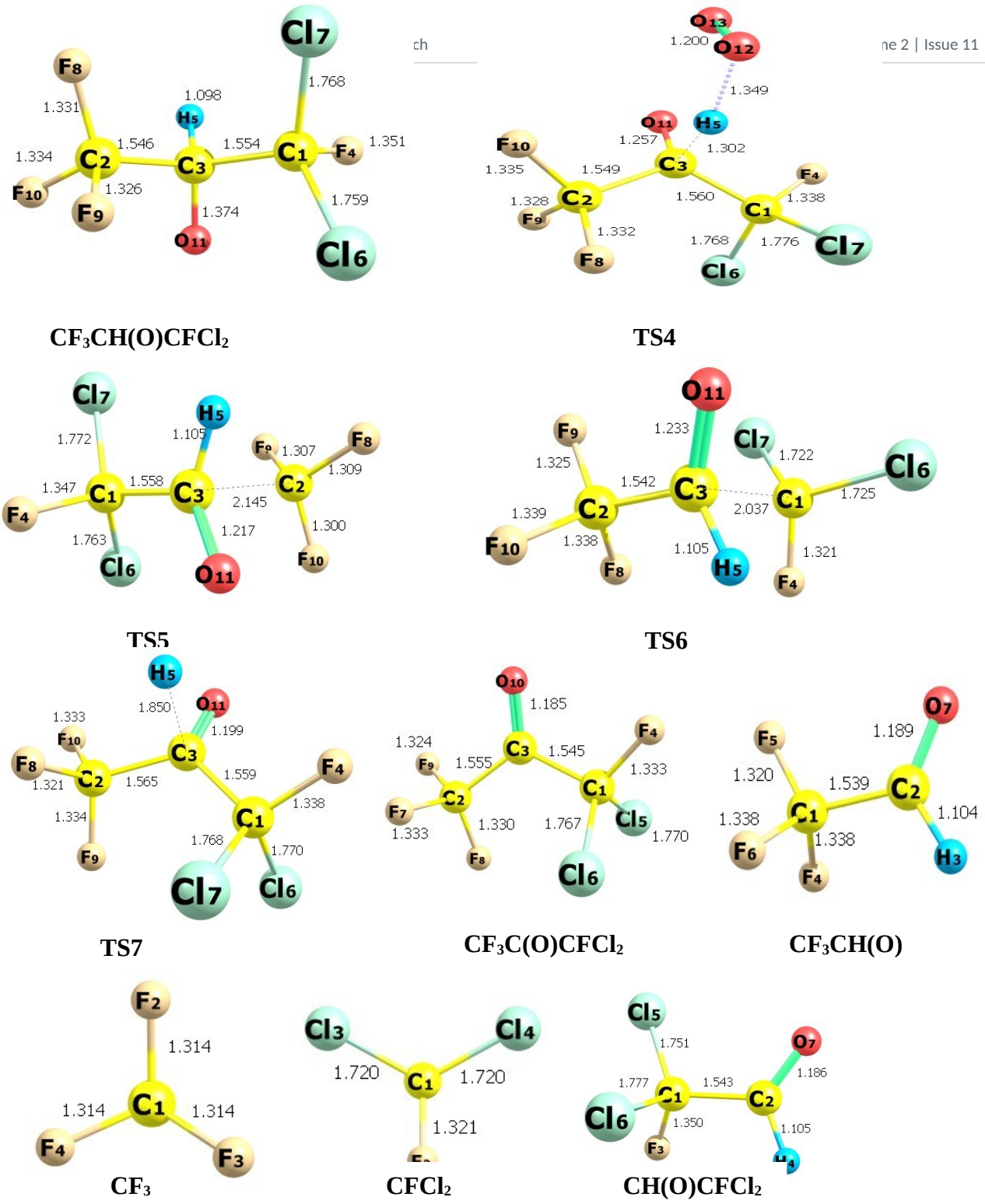

Fig. 4: Optimized geometries of product complexes and products at M06-2X/6-311+G(d,p) level.Bond lengths are in Angstroms.

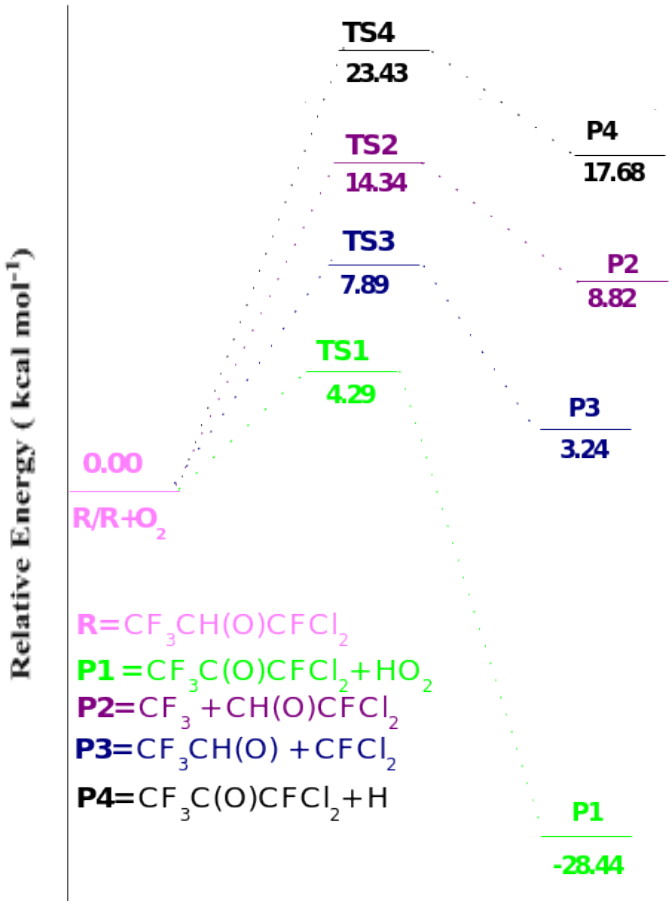

Fig. 5: Schematic potential energy diagram for the decomposition channels of alkoxy radical. Relative energies (in kcal mol^{-1}) with ZPE at M06-2X/6-311+G(d,p) level.